BIOAPATITE MADE FROM CHICKEN FEMUR BONE

#MONIKA ŠUPOVÁ, GRAŽYNA SIMHA MARTYNKOVÁ*, ZBYNĚK SUCHARDA

Institute of Rock Structure and Mechanics, Academy of Sciences of the Czech Republic (ASCR), V Holešovičkách 41, Prague, 182 09, Czech Republic
**Nanotechnology Centre, VŠB-Technical University of Ostrava, 17. listopadu 15/2172, Ostrava-Poruba, 708 33, Czech Republic*

#E-mail: supova@irsm.cas.cz

Submitted April 4, 2011; accepted July 3, 2011

Keywords: Bioapatite, Biocomposite, Bone, Hydroxyapatite, Nanoparticles

Nano-bioapatite (BAP) powder was successfully acquired from chicken femur bones via chemical treatment followed by calcination. The isolation of nano-bioapatite powder from chicken bone has not been published so far. The bioapatite powder was chemically and structurally characterized by elemental analysis (AAS), X-ray diffraction (XRD), transmission electron microscopy (TEM), and Fourier transform infrared spectroscopy (FTIR) techniques. The nano BAP powder showed needle-shaped morphology. The crystallite size distribution and specific surface area proved the nanostructured character of the sample. Chemical analysis together with FTIR spectrometry have demonstrated that the BAP powder was Ca-deficient with Na, Mg and carbonate substitutions that make the BAP suitable for application as a filler in biocomposites.

INTRODUCTION

Bone is a complex, composite material with inorganic and organic matrix. The inorganic part of the human bone has chemical and structural similarities with hydroxyapatite (HA) in the form of plate-shaped nanocrystals [1-3] that are 2-3 nm in thickness and tens of nanometers in length and width [1]. Human bones do not have a pure or stoichiometric HA, but incorporate many elements; some of them at the ppm level [4-6] and play a vital and selective role in the biochemical reactions associated with bone metabolism. Skinner [5] presented the overall range of bioapatite chemistry as $(Ca,Na,Mg,K,Sr,Pb,...)_{10}$ $(PO_4,CO_3,SO_4,...)_6$ $(OH,F,Cl,CO_3)_2$, whereas Cazalbou et al. [7] use $Ca_{8.3}\square_{1.7}$ $(PO_4)_{4.3}(HPO_4$ and $CO_3)_{1.7}(OH$ and $0.5CO_3)_{0.3}\square_{1.7}$ to indicate the extremely important role of structural carbonate in bone apatite (where □ is a vacancy). Ionic substitution can affect the crystal structure, crystallinity, surface charge, solubility and other vital properties, leading to major changes in the biological performance upon implantation.

As an alternative to processes for the preparation of synthetic apatite as composite nanofiller, mineral phase has been obtained from different natural sources. Nano hydroxyapatite powder was successfully synthesized from biowaste chicken eggshells by a calcination at high temperature (900°C) followed by reaction with phosphate solution [8, 9]. A similar technique however with lower using temperatures (200-350°C) has been used for hydroxyapatite preparation from different types of sea creatures, such as Indian coral [10], Australian coral [11], Sorites skeleton [12], Goniopora coral [13] and cuttlefish bone [14, 15]. Vecchio et al. have prepared biocompatible hydroxyapatite and Mg-substituted tricalcium phosphate from seashells [16] and sea urchin spines [17], respectively, by hydrothermal conversion.

Another possible source for obtaining bioapatite can be warm-blooded animal bones. Murugan et al. have demonstrated an easy, cost-effective approach to a reproducible processing of hydroxy-carbonate apatite scaffold from the chemically and thermally processed bovine bone without any extraneous ionic substitution but leaving only the natural trace elements. Xenogeneic bone procured from the slaughterhouse waste [18] and from cortical portion of bovine bone [19] was deproteinated by heat treatment. The FTIR spectra of raw bone and bone heated at 300°C indicated the presence of organic macromolecules whereas these disappeared in the samples heated at 500, 700 and 900°C, which suggested the removal of antigenic organic matters around 500°C and that low temperature treatment does not alter morphological and structural properties. They have used bone samples that were chemically treated and

preheated at 700°C for the preparation of fluoroapatite [20]. The fluoridation has been done in two ways: in the low-temperature method by reaction of the bone sample with HF, in the high-temperature method by grinding of the bone sample with NaF at 900°C. Emaldi et al. [21] have used a novel method to synthesize β-TCP/HAP biphasic ceramic scaffolds from natural cancellous bone. Bovine bone was calcined to remove the organic content. The remaining material was then soaked in P_2O_5 solution for different periods. P ions were doped into cancellous bone and reacted with hydroxyapatite to produce ß-tricalcium phosphate. This simple process can be employed to prepare different HAP/TCP ratios of bioceramics with a natural bone porous structure by changing the soaking time. Guizzardi et al. [22] have obtained bioapatite from horse compact bone by treating in a sodium hypochlorite solution for 10 days followed by calcination at 400°C.

In the present study we report an isolation of bioapatite (BAP) from chicken femur bone, which represents another alternative source of bone apatite, using a chemical and thermal deproteinating process. The isolation of nano bioapatite powder from chicken bone has not been published so far. The obtained bioapatite has been chemically and structurally characterized by AAS, FTIR and XRD. The character of bioapatite nanoparticles has been study by TEM.

EXPERIMENTAL

BAP powder was obtained using a chemical and thermal deproteinating process inspired by Murugan et al. [19]. The cortical chicken bones were heated with a 2 % NaCl aqueous solution at 150°C and pressure of 0.2 MPa in an autoclave, followed by disintegration of the sample in a mixer and degreasing in an acetone–ether mixture (ratio 3 : 2) for 24 hours. Bone samples were then treated with 4 % NaOH solution at 70°C for 24 hours. The chemically treated bone samples were calcined overnight at 500°C under atmospheric pressure and ambient humidity. The product was washed with deionized water and dried in an oven at 80°C.

Sodium and magnesium were determined by atomic absorption spectroscopy (Varian AA 240), phosphate by the photometric method (UV-VIS 500, Unicam) and calcium by the titration method. Specific gravity was determined pycnometrically in water.

The morphology of BAP particles was studied by transmission electron microscopy (TEM; microscope Tecnai G2 Spirit Twin). The sample was dispersed in diethylether and spread over a microscopic support and diethylether was left to evaporate. The support was a copper grid covered with a thin carbon film and the samples were observed at 120 kV in the bright field mode. The surface area was determined by the BET method (Sorptomatic 1990) with nitrogen as the adsorbate gas.

The X-ray diffraction (XRD) pattern of the final nanopowder was obtained with an X-Ray Powder Diffractometer D8 Advance (Bruker AXS, Germany) using Bragg-Brentano diffraction geometry with CoKα radiation (λ = 1.78Å) and a position sensitive VANTEC detector in the reflecting mode. Crystallite size and size distribution were calculated using software MudMaster [23] using the Warren-Averbach [24] approach.

Fourier transform infrared spectroscopy (FTIR) was done with Protégé 460 E.S.P. (Thermo-Nicolet, Inc., USA) over the range between 4000 and 400 cm^{-1} at 2 cm^{-1} resolution, averaging 32 scans by the KBr tablet technique. The CO_3^{2-} content was qualitatively determined from the infrared spectrum of BAP by comparing the extinction coefficient (E) of the 1450 cm^{-1} (carbonate) and 569 cm^{-1} (phosphate) peaks using the formula: $\%CO_3^{2-} = 13.5$ (E1450/E569) - 0.2 [19], the CO_3^{2-} content was also quantitatively determined using an elemental analysis by a CHNS/O microanalyzator Flash FA 1112 Thermo Finnigan (Carlo Erba).

RESULTS AND DISCUSSION

Results of the chemical analysis of the BAP sample are summarized in Table 1. As can be seen from Table 1, the BAP sample contains 0.71 and 0.80 wt. % of magnesium and sodium, respectively. Substitution of sodium for calcium balances the negative charge caused by the substitution of phosphate by carbonate [25]. Presence and concentration of carbonate have been determined by FTIR method which is described below. The amount of magnesium ions associated to apatite is usually much higher than that incorporated into its crystalline structure, where it can substitute for calcium at most up to about 10 at.% [26, 27], and it is mainly adsorbed on the apatite crystal surface [28]. Owing to these substitutions the Ca/P molar ratio is smaller (1.64) than 1.67 that is typical for stoichiometric hydroxyapatite. This fact becomes evident from the value of specific gravity 2.864 for BAP compared to 3.080 for stoichiometric hydroxyapatite.

A transmission electron micrograph of the BAP nanoparticles is shown in Figure 1. Generally, the nanoparticles appear to have a needle shape with heights of

Table 1. Characterization of BAP sample.

Type of apatite	Specific surface area (m^2/g)	Pore specific volume (cm^3/g)	Mean elements and carbonate concentrations (wt.%)				Ca/P molar ratio	Specific gravity
			Mg	Na	CO_3^{2-} exp.	CO_3^{2-} el.an.		
BAP	73.3	0.28	0.71	0.80	3.11	3.25	1.64	2.864

~20 nm to 90 nm and diameters of ~13 nm to 20 nm. The average values of the specific surface area and pore specific volume determined by BET were 73.3 m^2/g and 0.28 cm^3/g, respectively (Table 1). This value of specific surface area demonstrates the nano nature of BAP particles which is approximately in agreement with data reported on a commercial website (Berkeley Advanced Biomaterials, Inc., CA) where particles with sizes 100 nm have specific surface area 50-70 m^2/g. In a hydroxyapatite reference material a specific surface area of 18.3 m^2/g^{-1} corresponded to particles with height of 100-300 nm and diameter of 50-150 nm [29].

X-ray diffraction analysis served for material crystallinity estimation. The diffraction pattern of BAP (Figure 2) represents typical broadened peaks of nanocrystalline material. The crystallite size Lc was calculated using the (002) basal diffraction peak 30.15° 2Θ (in figure $d = 0.34$ nm), because the clear profile and independence of the line is favorable. The area-weighted mean crystallite size <Lc> was calculated according to the theory of Warren and Averbach [24] from the distribution, <Lc> = 25 nm. The crystallite size distribution curve has two maxima (Figure 3) and the calculated log-normal distribution (solid line) fits the character of the BAP distribution. The majority of crystallites are in the range 12 to 40 nm, with an asymmetry towards the smaller sizes. Below 10 nm the amount of crystallites is negligible. Larger domains are represented with sizes around 60 nm. However, the crystallites are rather small and uniform, which is advantageous for further evaluation of composite and applications. For comparison, the average crystallite size of human bone in the c-axis direction, studied by Handschin and Stern [30], has been determined as 28 nm within the age group 0-25, to reach a constant average domain size of 34 nm within the age group 30-80. The crystallite size is related to the resorption of bioapatite in bone. Bone undergoes constant remodeling [31]. Weng et al. [32] have found that more amorphous hydroxyapatite coatings were soluble in simulated body fluid and were resorbed when introduced into the body.

The chemical functionality of BAP was determined from its FTIR spectrum (Figure 4). The spectrum shows a weak broad band ranging between 3550 and 3350 cm^{-1}, corresponds to strongly adsorbed and/or bound H_2O [33]. H_2O bands were also observed at 1634 cm^{-1}. The weak 3564 cm^{-1} band corresponds to the OH^- group, another band corresponding to OH^- groups at 635 cm^{-1} was not detected, which is in agree-ment with published data [34, 35] that nanocrystalline apatite contains little or no OH^- groups. The low portion of OH^- groups in the bone apatite thus would favor its dissolution and resorption [35]. A strong band of PO_4^{3-} group is visible at 1039 cm^{-1} (stretching vibration) and bands at 590-610 cm^{-1} region are due to deformation vibration of PO_4^{3-} ions. Bands pertain to the CO_3^{2-} functional group at ~1500 and 870 cm^{-1}, indicating the substitution of CO_3^{2-} ions into the apatite. The CO_3^{2-} peak at 1550 cm^{-1} assigned to the A- type (CO_3^{2-} is substituted for OH^-) was not detected owing to the absence of OH^-. The band at 870 cm^{-1} indicates a B-type carbonate substitution (part of the PO_4^{3-} groups is replaced by CO_3^{2}). The amount of CO_3^{2-} estimated by a FTIR method using an equation given in the Experimental chapter was found to be 3.11 wt.%, which corresponds well with the results determined by the CHNS/O analyzer - 3.25 wt.%. Other authors´ studies also have shown that the carbonate concentration in apatite correlates positively with its solubility [4]. Thus, both the smaller crystallite size and higher carbonate concentration account for the much greater solubility and resorbability [31].

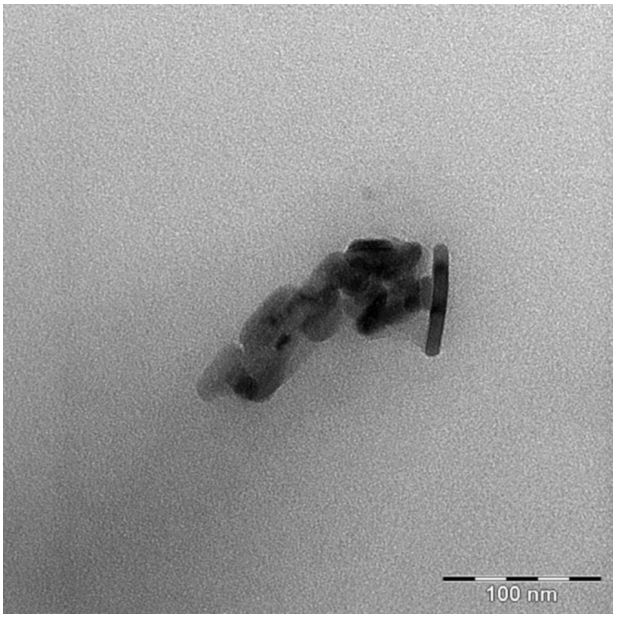

Figure 1. TEM image of BAP sample.

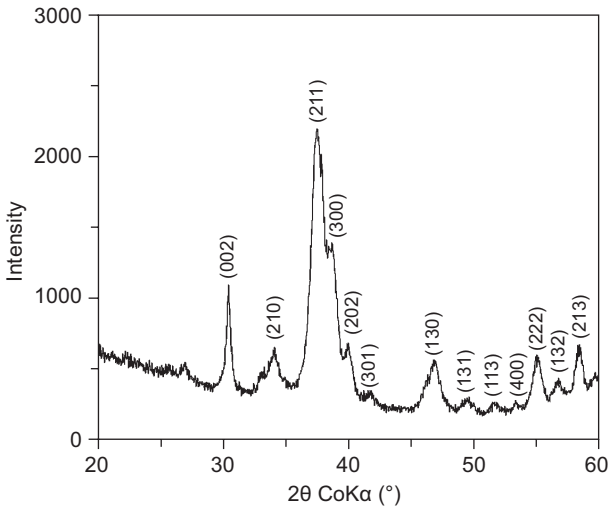

Figure 2. X-ray diffraction pattern of BAP denoted with Miller indices.

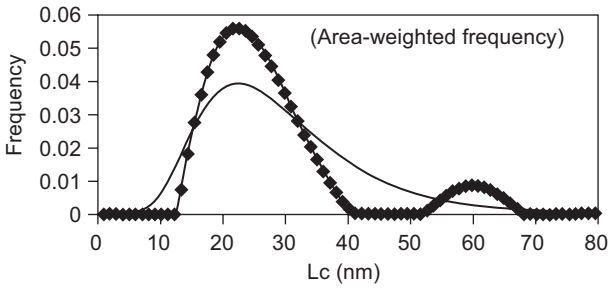

Figure 3. Crystallite size distribution of BAP, the solid curve given in the distribution is for a theoretical lognormal curve that has been calculated from the measured distribution.

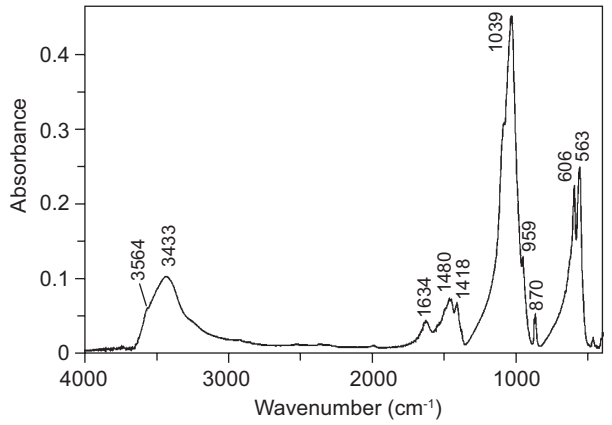

Figure 4. Baseline-corrected FTIR spectrum of BAP sample.

CONCLUSIONS

In this study, chicken femur bone was used to isolate nano-bioapatite powder via chemical treatment followed by calcination. The nano BAP particles showed needle-shaped morphology. The crystallite size distribution determined using the Warren-Averbach approach and specific surface area determined by BET proved the nanostructured character of the sample. Values of specific gravity and Ca/P molar ratio together with chemical analysis and FTIR spectrometry have demonstrated that BAP sample was Ca-deficient with Na, Mg and carbonate substitutions. All these properties mentioned above are related to good solubility and resorbability, which are very important for bone remodeling. The present study shows that chicken femur bone can be effectively utilized for the preparation of nano-bioapatite powders as potential filler to biocomposites.

Acknowledgements

The authors wish to acknowledge the GAČR 106/09/1000 (Grant agency of the Czech Republic) project for financial supports, Alena Jandečková (Institute of Rock Structure and Mechanics, Academy of Sciences, Czech Republic) for BET analysis and Dr. Miroslav Šlouf (Institute of Macromolecular Chemistry, Academy of Sciences, Czech Republic) for TEM analysis.

References

1. Weiner S., Wagner H.D.: Annu. Rev. Mater. Sci. *28*, 271 (1998).
2. Eppell S.J., Tong W., Lawrence J., Kun L., Glimcher M.J.: J. Orthop. Res. *19*, 1027 (2001).
3. Veis A.: Science *307*, 1419 (2005).
4. Elliott J.C.: Phosphates: Geochemical, Geobiological and Material Importance, Reviews in Mineralogy and Geochemistry, Mineralogical Society of America, Washington DC 2002.
5. Skinner H.C.W.: Biominerals. Mineralogical Magazine *69*, 621 (2005).
6. LeGeros R.Z.: Hydroxyapatite and Related Materials, Boca Raton:CRC Press 1994.
7. Cazalbou S., Combes C., Eichert D., Rey C.: J. Mater. Chem. *14*, 2148 (2004).
8. Rivera E.M., Araiza M., Brostow W., Castaño V.M., Díaz-Estrada J.R., Hernández R., et al.: Mater. Lett. *41*, 128 (1999).
9. Sanosh K.P., Chu M.Ch., Balakrishnan A., Kim T.N., Cho S.J.: Mater. Lett. *63*, 2100 (2009).
10. Sivakumar M., Sampath Kumar T.S., Shantha K.L., Panduranga Rao K.: Biomaterials *17*, 1709 (1996).
11. Hu J., Russell J.J., Ben-Nisan B., Vago R.: J. Mater. Sci. Lett. *20*, 85 (2001).
12. Xu Y., Wang D., Yang L.: Mater. Character. *47*, 83 (2001).
13. Ripamonti U., Crooks J., Khoali L., Roden L.: Biomaterials *30*, 1428 (2009).
14. Rocha J.H.G., Lemos A.F., Agathopoulos S., Valério P., Kannan S., Oktar F.N., et al.: Bone *37*, 850 (2005).
15. Rocha J.H.G., Lemos A.F., Agathopoulos S., Kannan S., Valério P., Ferrara J.M.F.: J. Biomed. Mater. Res. A. *77*, 160 (2006).
16. Vecchio K.S., Zhang X., Massie J.B., Wang M., Kim C.W.: Acta Biomaterialia *3*, 910 (2007).
17. Vecchio K.S., Zhang X., Massie J.B., Wang M., Kim C.W.: Acta Biomaterialia *3*, 785 (2007).
18. Murugan R., Panduranga Rao K., Sampath Kumar T.S.: Bull. Mater. Sci. *26*, 523 (2003).
19. Murugan R., Ramakrishna S., Panduranga Rao K.: Mater. Lett. *60*, 2844 (2006).
20. Murugan R., Panduranga Rao K., Sampath Kumar T.S.: Mater. Lett. *57*, 429 (2002).
21. Emadi R., Roohani Esfahani S.I., Tavangarian F.: Mater. Lett. *64*, 993 (2010).
22. Guizzardi S., Montanami C., Migliaccio S., Strocchi R., Solmi R., Martini D., et al.: J. Biomed. Mater. Res. B. *53*, 227 (2000).
23. Eberl D.D., Drits V., Srodon J., Nüesch R.: U.S. Geological Survey Open File Report. *96* (1996).
24. Warren B.E., Averbach B.L.: J. Appl. Phys.: *21*, 595 (1953).
25. Barralet J., Best S., Bonfield W.: J. Biomed. Mater. Res. A. *41*, 79 (1998).
26. Bigi A., Falini G., Foresti E., Gazzano M., Ripamonti A., Roveri N.: Acta Crystallogr. B. *52*, 87 (1996).

27. Mayer L., Schlam R., Featberstone J.D.B.: J. Inorg. Biochem. *66*, 1 (1997).
28. Bertoni E., Bigi A., Cojazzi G., Gandolfi M., Panzavolta S., Roveri N.: J. Inorg. Biochem. *72*, 29 (1998).
29. Markovic M., Fowler B.O., Tung M.S.: J. Res. Natl. Inst. Stand. *109*, 553 (2004).
30. Handschin R.G., Stern W.B.: Bone *16*, 355S (1995).
31. Wopenka B., Pasteris J.D.: Mat. Sci. Eng. C-Bio S. *25*, 131 (2005).
32. Weng J., Liu X., Li X., Zhang X.: Biomaterials *16*, 39 (1995).
33. Elliott J.C.: *Structure and chemistry of the apatites and other calciumorthophosphates*, Elsevier, Amsterdam 1994.
34. Pasteris J.D., Wopenka B., Valsami-Jones E.: Elements *4*, 97 (2008).
35. Pasteris J.D., Wopenka B., Freeman J.J., Rogers K., Valsami-Jones E., van der Houwen J.A.M., et al.: Biomaterials *25*, 229 (2004).